Supplement for: Depth-varying azimuthal anisotropy and mantle flow in the Patagonian slab window

Hannah F. Mark * [1,2], **Douglas A. Wiens** [3], **Walid Ben-Mansour** [3], **Zhengyang Zhou** [4]

[1]Department of Geology and Geophysics, Woods Hole Oceanographic Institution, Woods Hole, MA, USA, [2]Lamont Doherty Earth Observatory of Columbia University, Palisades, NY, USA, [3]Department of Earth, Environmental, and Planetary Sciences, Washington University in St. Louis, St. Louis, MO, USA, [4]College of Earth, Ocean, and Atmospheric Sciences, Oregon State University, Corvallis, OR, USA

S1 Contents

This supplement contains a table of information on prior distributions for Markov chain Monte Carlo (MCMC) inversion (Table S1), figures comparing the isotropic component of this study's velocity model to that of Mark et al. (2022) (Figures S1 to S5), figures comparing sediment and crustal thickness between the same two models (Figures S6 and S7), a figure showing the uncertainty in anisotropy amplitudes from MCMC (Figure S8), and a figure illustrating the outputs of the MCMC code and what exactly is being fit in that inversion (Figure S9).

Parameter	Prior range
Crust velocity splines	± 10%
Crust cos/sin coefficients	± 10%
Mantle velocity splines	± 10%
Mantle cos/sin coefficients	± 10%
Sediment thickness	± 3 km
Crustal thickness	± 5 km
Sediment top/bottom velocities	± 0.5 km/s

Table S1 Parameter search ranges for Markov chain Monte Carlo inversion.

*Corresponding author: hmark@ldeo.columbia.edu

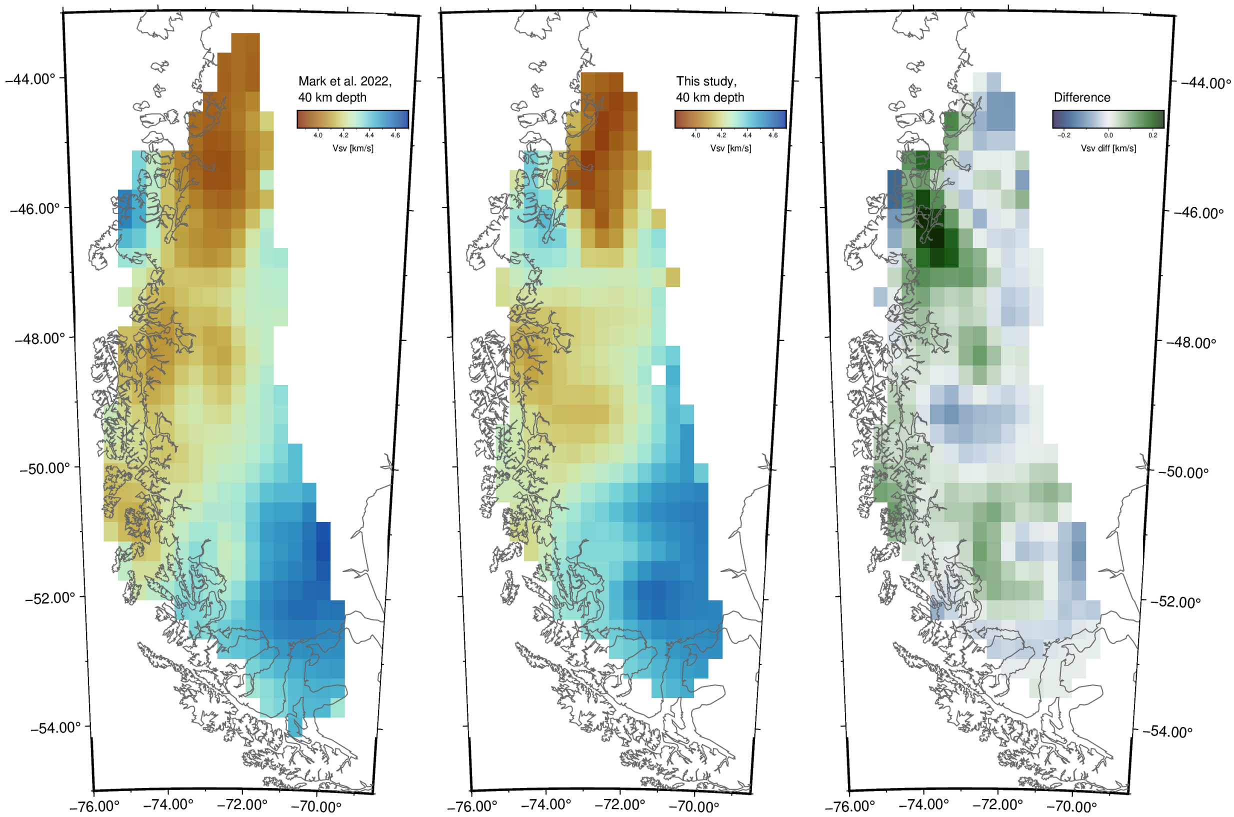

Figure S1 Comparison of isotropic background $V_s v$ from this study and the model of Mark et al. (2022). Velocities shown are at 40 km depth. Color scales are the same in the left and center panels.

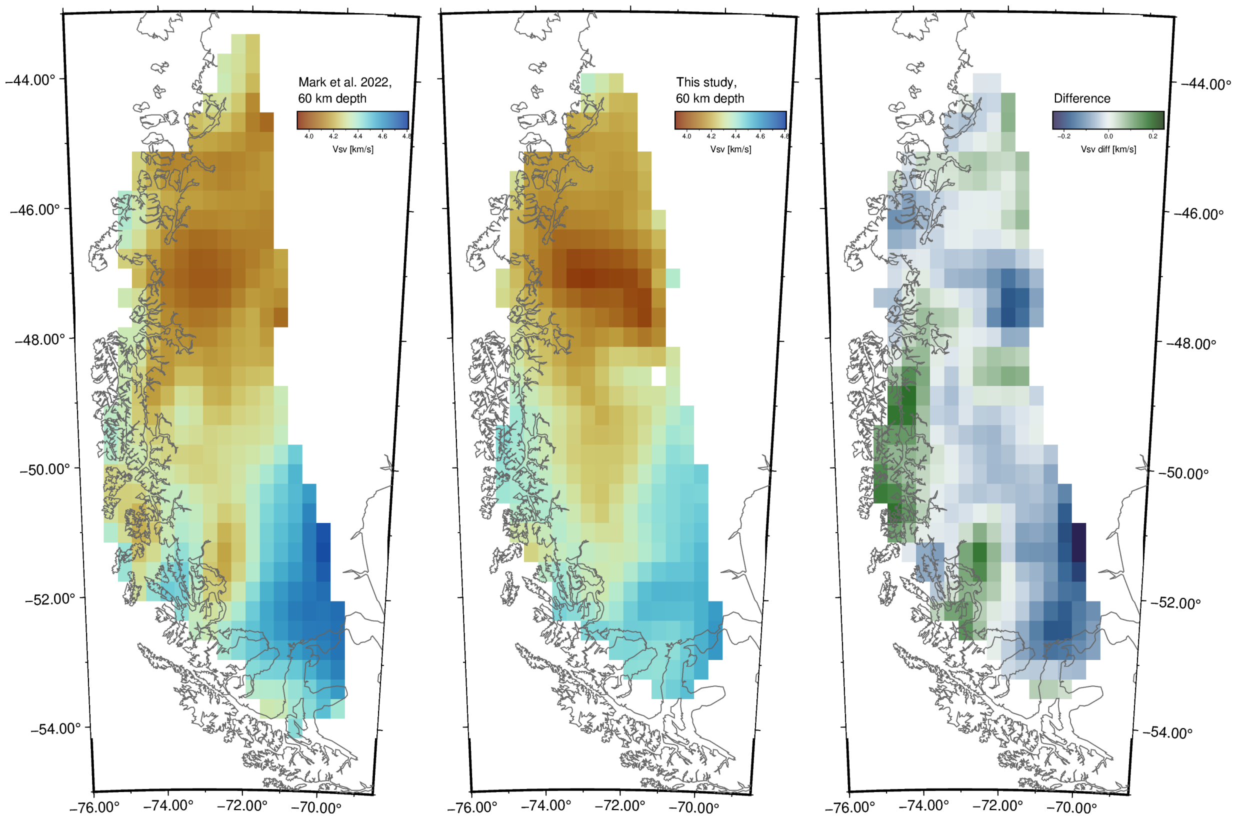

Figure S2 Comparison of isotropic background $V_s v$ from this study and the model of Mark et al. (2022). Velocities shown are at 60 km depth. Color scales are the same in the left and center panels.

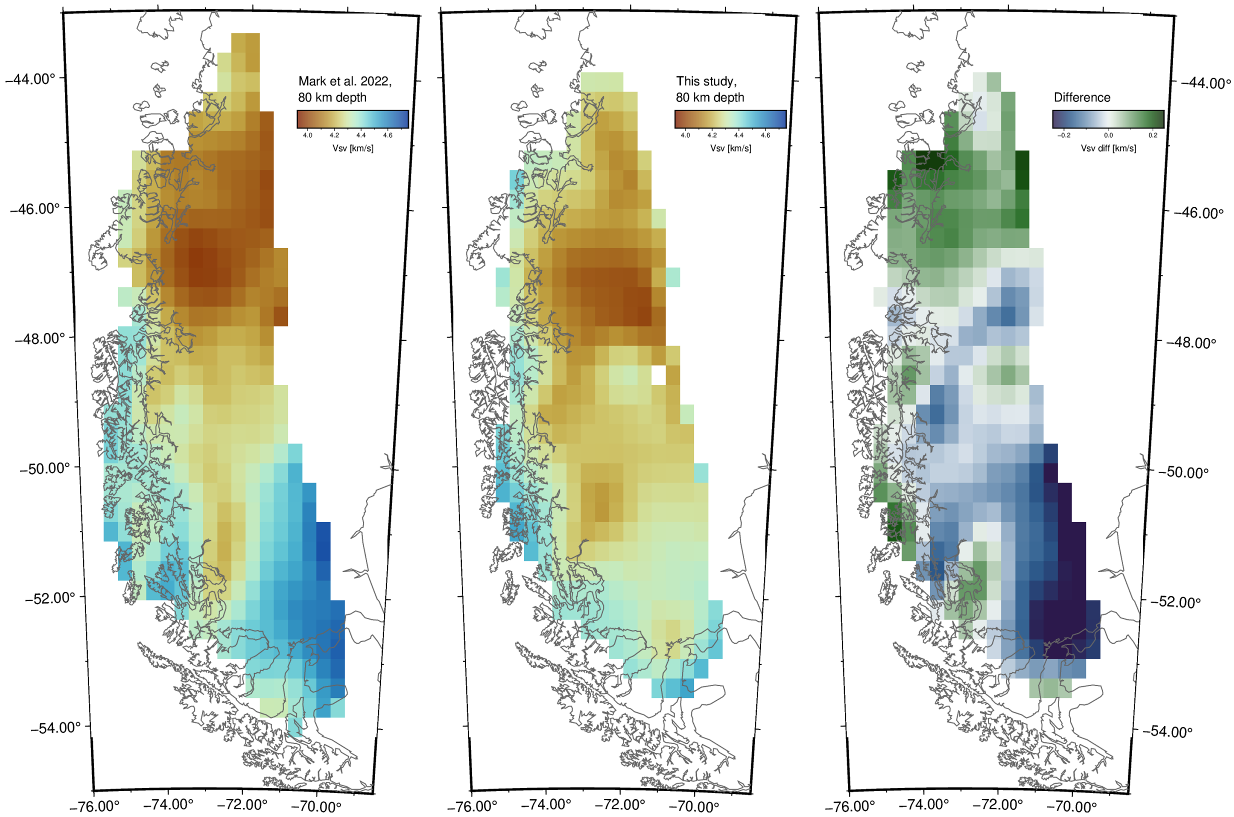

Figure S3 Comparison of isotropic background $V_s v$ from this study and the model of Mark et al. (2022). Velocities shown are at 80 km depth. Color scales are the same in the left and center panels.

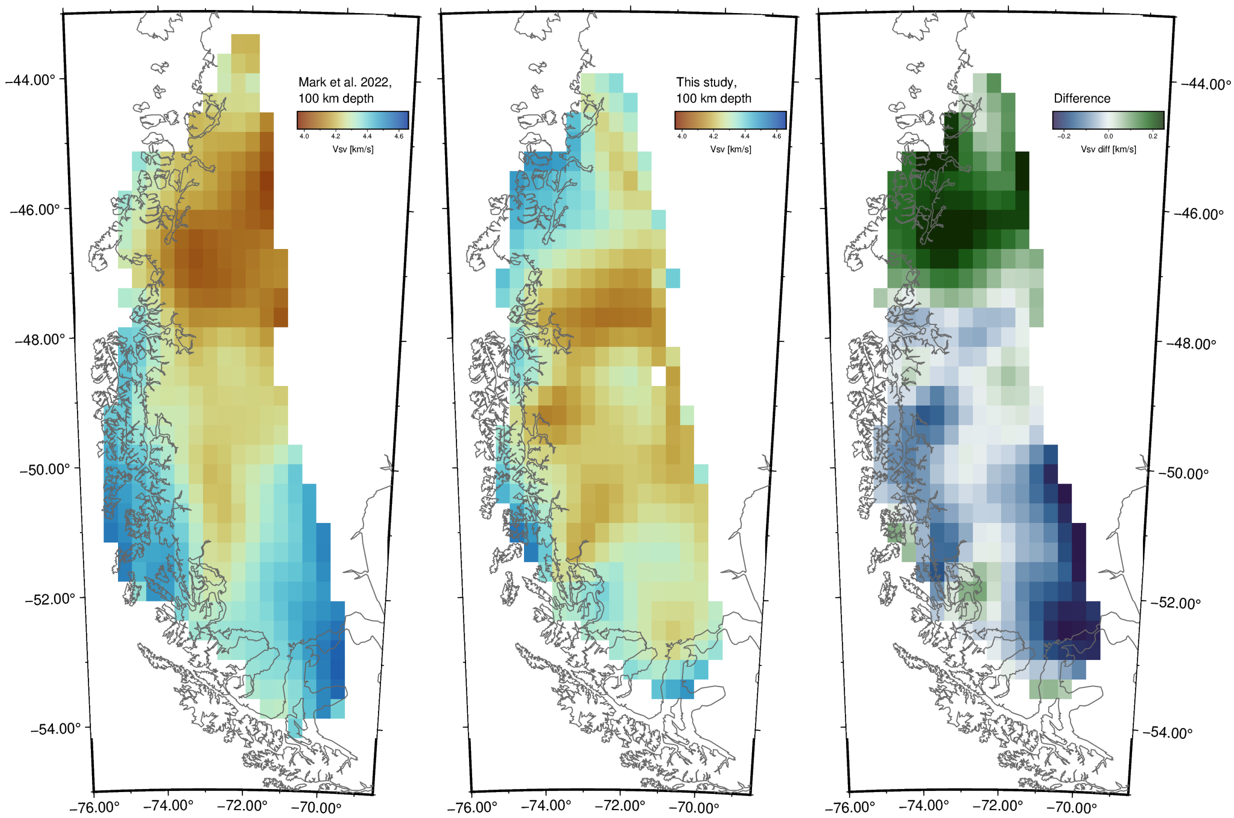

Figure S4 Comparison of isotropic background $V_s v$ from this study and the model of Mark et al. (2022). Velocities shown are at 100 km depth. Color scales are the same in the left and center panels.

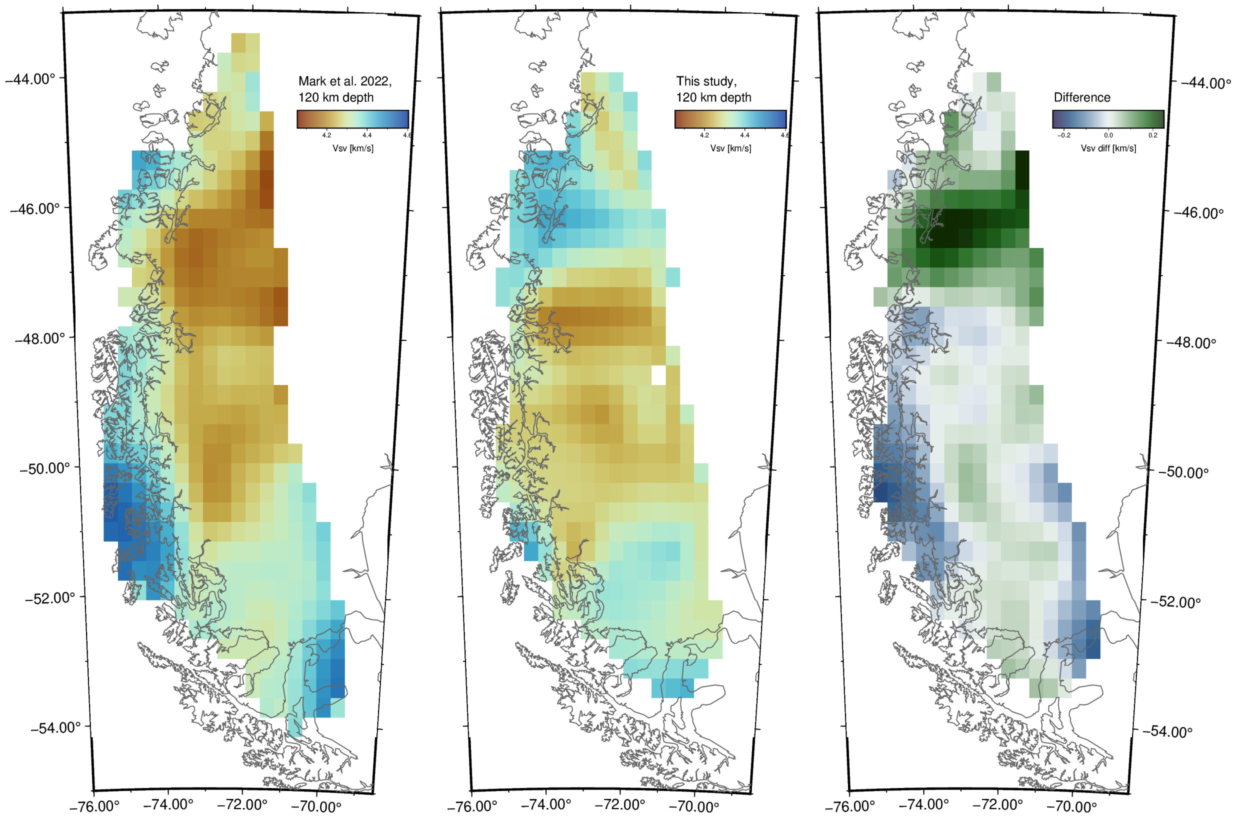

Figure S5 Comparison of isotropic background V_sv from this study and the model of Mark et al. (2022). Velocities shown are at 120 km depth. Color scales are the same in the left and center panels.

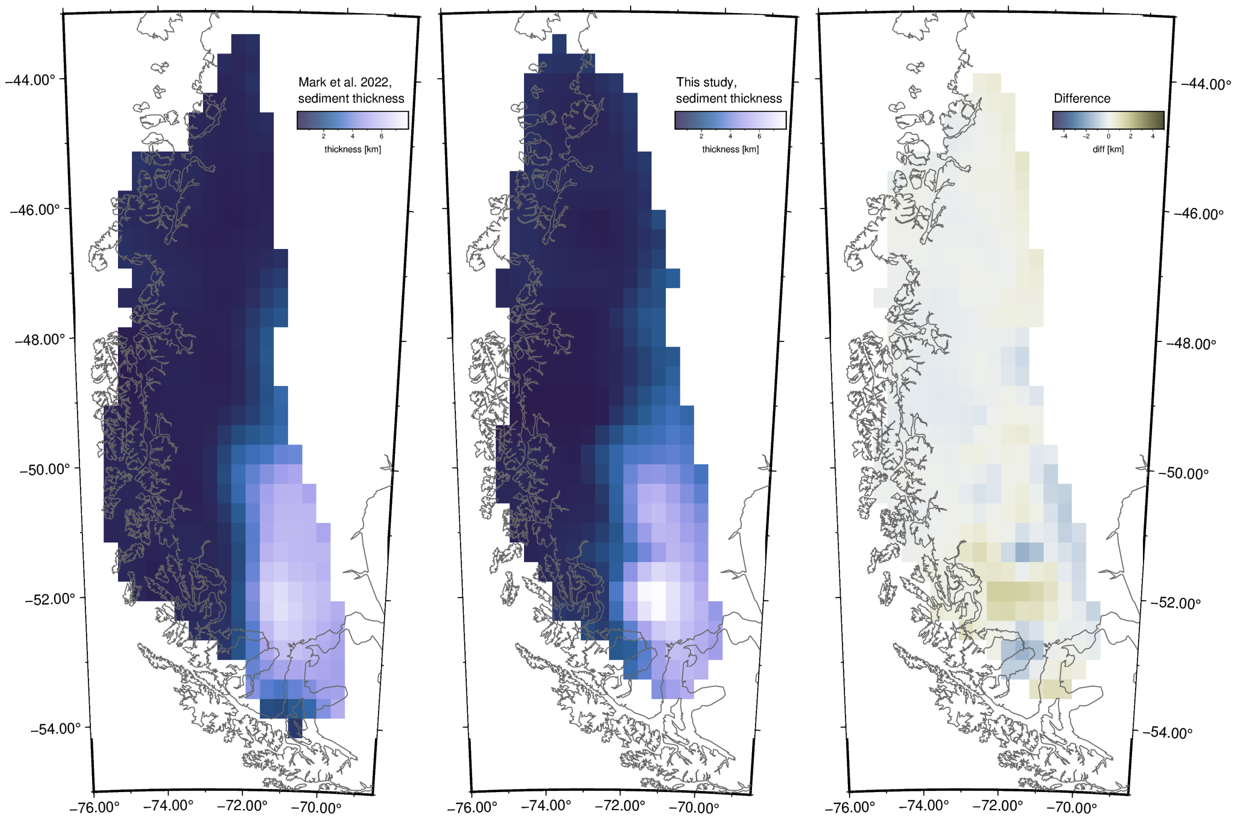

Figure S6 Comparison of sediment thickness from this study and the model of Mark et al. (2022). Color scales are the same in the left and center panels.

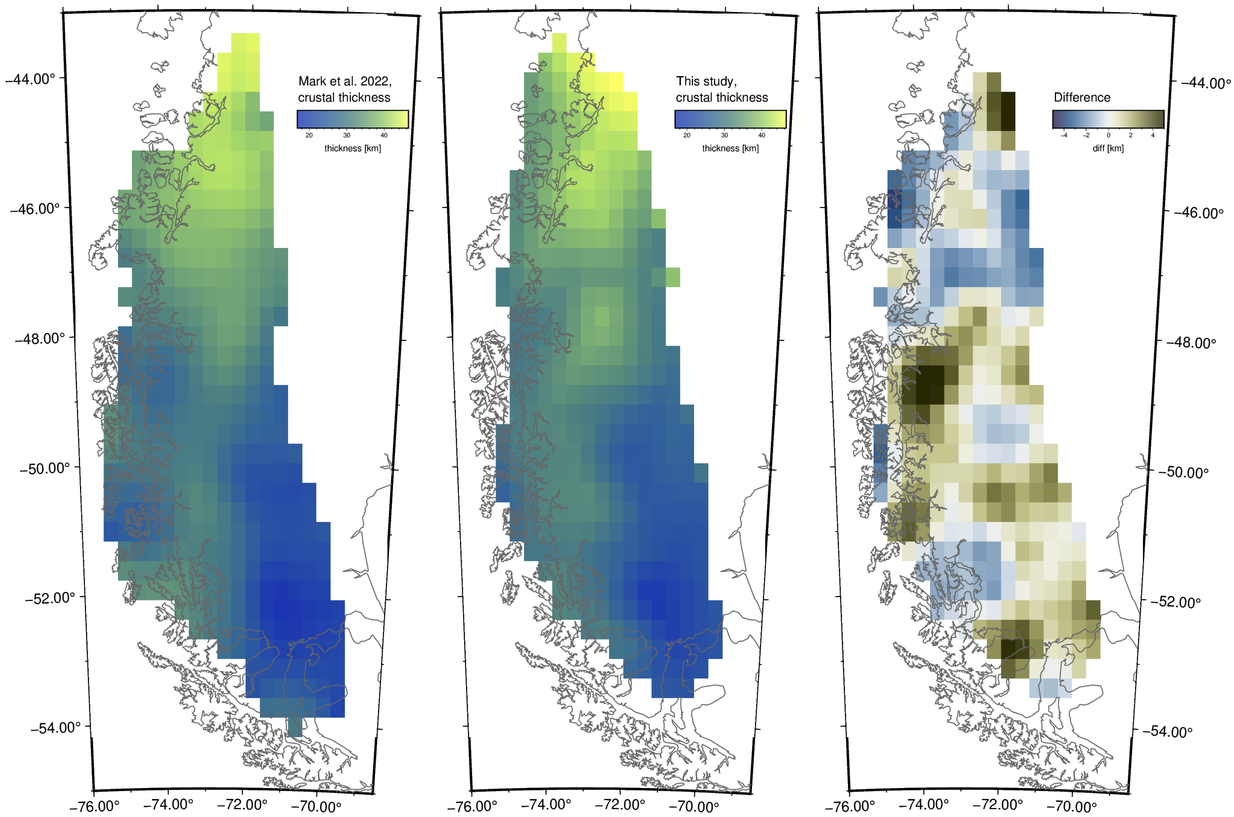

Figure S7 Comparison of crustal thickness from this study and the model of Mark et al. (2022). Color scales are the same in the left and center panels.

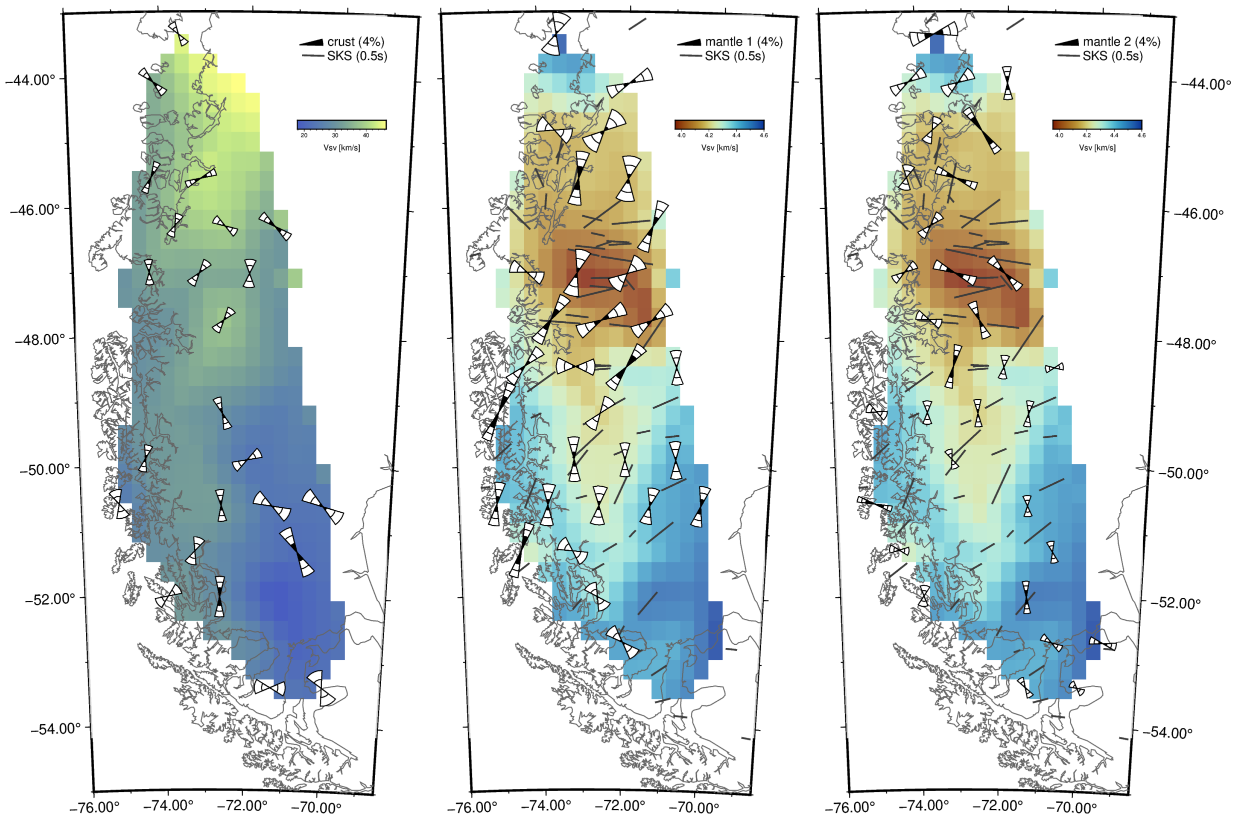

Figure S8 Anisotropy magnitude uncertainties for the crust, upper mantle sub-layer, and lower mantle sub-layer. Each anisotropy measurement is shown by a bow tie symbol where the inner black portion is the minimum amplitude, the outer white portion is the maximum amplitude, and the black line across the white section is the mean value. The backgrounds are crustal thickness (left panel) and isotropic velocity at 60 km depth (center and right panels). Shear wave splits from Ben-Mansour et al. (2022) are plotted as grey lines in the center and right panels.

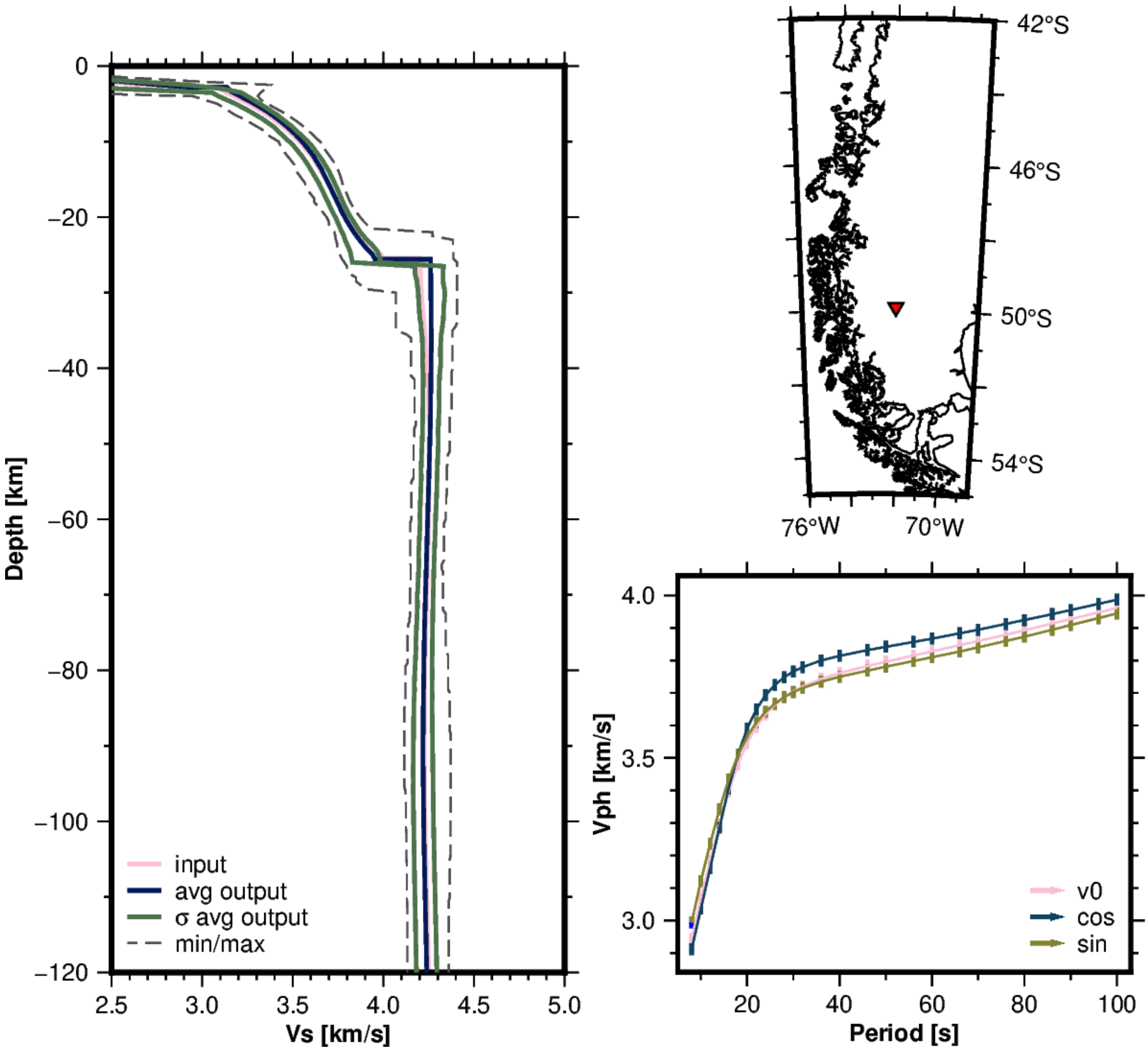

Figure S9 Results of the Bayesian inversion for the point 49.912S, 72.000W. The left panel shows velocity as a function of depth for the input model, the average of accepted outputs, one standard deviation of that average, and the full range of acceptable models. The top right map shows the location for this pointwise inversion. The bottom right shows the dispersion curves that were fit in the inversion: v0 for the isotropic component, and cos/sin curves which incorporate the 2θ cosine and sine terms at each period. Bars show the input uncertainty for each phase velocity, and lines show the average accepted model from MCMC inversion.

References

Ben-Mansour, W., Wiens, D. A., Mark, H. F., Russo, R. M., Richter, A., Marderwald, E., and Barrientos, S. Mantle Flow Pattern Associated With the Patagonian Slab Window Determined From Azimuthal Anisotropy. *Geophysical Research Letters*, 49(18), 2022. doi: 10.1029/2022GL099871.

Mark, H. F., Wiens, D. A., Ivins, E. R., Richter, A., Ben Mansour, W., Magnani, M. B., Marderwald, E., Adaros, R., and Barrientos, S. Lithospheric Erosion in the Patagonian Slab Window, and Implications for Glacial Isostasy. *Geophysical Research Letters*, 49(2), Jan. 2022. doi: 10.1029/2021GL096863.